FT-NIR Review of Application Limits and Application to Chitosan Characterization

by

Athar Alhulaymi

Submitted in partial fulfillment of the requirements

for the Degree of Master of Applied Science

at

Dalhousie University

Halifax, Nova Scotia

March 2017

To my family, friends, and mentors

I am energized by your endless love and support

Table of Contents

List of Tables:

List of Figures:

Abstract:

This thesis reviews recent applications of NIR spectroscopy, specifically focusing on O-H, N-H and C-H bonds found most commonly in water, alcoholic beverages, proteins and sugars, and identifies practical errors associated with this measurement method. As part of this work, the degree of deacetylation (DD) of chitosan was experimentally characterized by NIR in comparison to other analytical methods. Chitosan is a natural derivative of chitin that is mostly found in crustaceans. It possesses unique biological properties, and has been successfully applied in food additives, water clarification, drug delivery systems, and biomaterials. The biological properties rely upon the degree of deacetylation (DD): the ratio of free amino groups to acetyl groups within the chitosan molecule. The DD is considered the most important chemical characteristics due to its direct influence on functionality of chitosan, and is measured traditionally using acid-base or potentiometric titration. This work explores the direct measurement of DD for chitosan powders using FT-NIR spectroscopy, providing a fast analysis method, which does not require significant sample preparation. The developed method was capable of determining DD to within +-0.4% for samples between 80 and 100% DD.

List of Abbreviations Used:

FT- NIR spectroscopy	Near- Infrared spectroscopy
DD	Degree of deacetylation
UV-vis spectroscopy	Ultraviolet-visible spectroscopy
IR spectroscopy	Infrared spectroscopy
N=N	Sodium azide
O-H	Hydroxyl group
C=O	Carbonyl function group
N-H	Amine group
CONHR	Functional group of phenylalanine
K	Potassium
P	Phosphorus
Mg	Magnesium
Ca	Calcium
5-FU	Anti-neoplastic
PBS	Phosphate-buffered saline
HCl	Hydrochloric acid
NaOH	Sodium hydroxide

Acknowledgement

All praises and thanks are to Allah, the Lord of the worlds, the most beneficent, the most merciful for helping me accomplish this work. May Allah reward those who contributed in fruition of this work.

I would like to thank my supervisor Dr. Adam Donaldson for his encouragement, enthusiastic attention, kind support, critical discussions, valuable advice and guidance.

My appreciation is extended to the members of committee, Dr. Amyl Ghanem, Dr. Jean-Francois Bousquet, and Dr. Jan Haelssig, thank you for the feedback. A special thanks is also extended to Dr. Ghanem for her kind soul and giving me the opportunity to work with her.

Finally, special recognition goes out to my family, for their support, encouragement and patience during my study.

1 Introduction

The present work provides an introduction to vibrational spectroscopy, particularly near-infrared radiation (NIR) spectroscopy, shedding light on its basic principle. A detailed discussion of the results and applications of NIR will be the main focus in this thesis. This work reviews the diverse applications of NIR in different fields. Working through spectroscopic analysis and studying the experimental method, the change in the chemical structure of the sample can be defined and the minimum concentration NIR can be used to detect is inferred to establish a list of the chemical concentrations and wavenumbers for a wide variety of chemical compounds.

An experiment was made to support the claim of FT-NIR as a fast, non-destructive, and precise technique. The aim of this experiment was to use FT-NIR spectroscopy to characterize the degree of deacetylation (DD) of chitosan in powder form. Different aspects were considered during testing of the DD using four samples such as vial position, powder mass, and the vial itself with the cap on. These aspects have minimum impact on the obtained results.

The broad objective of this thesis is to review and gain better understanding of the applications of NIR, identifying the minimum amount of different materials that NIR can accurately detect. More explicitly using NIR spectroscopy to determine the degree of deacetylation (DD) of chitosan in powder form with no processing.

This chapter introduces the concept of NIR absorption, providing a definition of Near-infrared radiation and the general properties of this technique. The next section reviews mostly the historical development of NIR including its discovery and the revolutionary

period. Subsequently, details of the basic principle of vibrational spectroscopy particularly NIR will be provided as well as the vibration modes associated with dipole moment in order to cause absorption in NIR spectral range.

1.1 Background

Near-infrared radiation is the region beyond the visible red light (4000-12820 cm^{-1}). It was discovered by William Herschel in the 1800s, where he used a prism to separate the electromagnetic spectrum and noticed increasing temperature beyond the visible light (Frensh, 2010). In the beginning, NIR was rarely used due to the difficulty in interpreting the overlapping bands. In the current time, Near-infrared spectroscopy is considered to be an efficient method of analysis in the industrial sector. It is a new non-destructive technique, suiTable for the analysis of variable forms of different materials whether it is a solid, liquid, or biotechnological pharmaceutical (Roggo, 2007). The main function of NIR spectroscopy is to detect a certain functional group or chemical bond found in organic and/or inorganic materials. Most of the molecules absorb in the NIR region, some of them give a strong signal such as O-H in water, C-N, N-H, and O=C in organic matters (Rinnan & Rinnan, 2007). Accordingly, NIR has contributed widely to various fields such as pharmaceutical and biomaterial applications. Furthermore, NIR is also used in quality control, material screening, and process analytical applications (Coates. 1998). Near-infrared spectroscopy combines some of the qualities of both UV-vis and IR, distinguishing it from other spectrum devices since the NIR region starts where the UV-vis region ends and it is a part of IR region. The spectral region of UV-vis is 10 to 780 nm, which is mostly used to detect the concentration of different molecules. In short, the way that UV-vis works depends strongly on the amount of absorbed light. Once the light falls on the sample, it

absorbs a specific wavenumber of light (each wavenumber has a special color), which leads the sample to appear in complementary color as shown in the Figure 1-1 (Owen, 2002). However, in some cases where the sample is colorless, near-infrared spectral region is used as a part of UV-vis spectroscopy. The second method is IR spectroscopy that has a finger print region (mid-infrared region, 2800-4000 cm^{-1}) mostly suitable to detect functional groups in organic compounds. All peaks in this region are considered to be fundamental. Also, the near-infrared region is used occasionally for the same purpose as shown in Table 1-1 (Enjalbert & Tams, 2009). The peaks in this region are called combination or vibrational which occur based on the presence of the fundamental peaks in mid-infrared region.

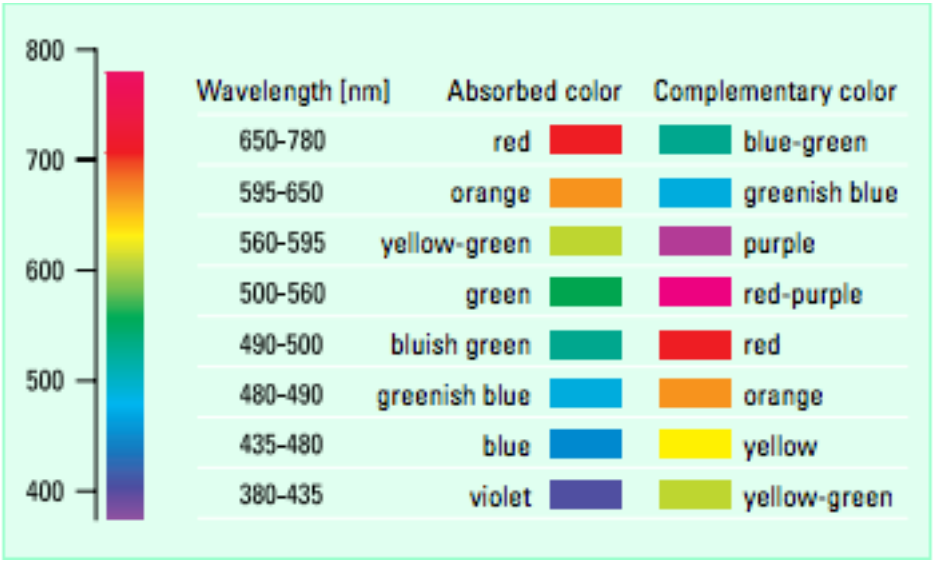

Figure 1-1: Absorbance and complementary colors (Owen, 2002)

Table 1-1: Wavenumbers of functional groups (Thermo Scientific, 2012).

BOND	**Mid-IR region**	**Near-infrared region Wavenumber (cm^{-1})**				**Combination**
		1st overtone	2nd overtone	3rd overtone	4th overtone	
O-H	3650-3200	7000	10500	12500-14000		5000
C-H	3300-2700	6000	8500-9000	11000	13000	
N-H	3500-3300	6750	9000-10000	11000-12500		4750-5000
C≡N	2260-2220	6250				4347
C≡C	2260-2100					4700-4900
C=C	1680-1600		9090-10000	12500		
C=N	1650-1550			1111		5263
C=O	1780-1650	5000-5263	5550-6600	1100-1200	12450	

Near-infrared spectroscopy is one of the three main branches of spectroscopy: mid-infrared (finger print region) and Raman. Before going further in the history of NIR, it is worth mentioning where the idea of NIR came from. The theory of separated light, diffraction and refraction started in the mid-17th century, which later were linked with the development of spectroscopy. The first attempt was by Sir Isaac Newton in 1666. He conducted a successful experiment and proved that using a pair of glass prisms strictly directed to the sunlight can separate the white light. By proving that, he revoked a stereotype of adding colors to the light while using a prism to separate it. One-hundred fifty years later, William Hyde Wollaston observed the first spectral line in 1802, building on Newton's experiment by using a narrow slit for greater accuracy. In 1814 a German glassmaker named Joseph von Fraunhofer made the first spectroscope. He observed the

spectra of various flames coming from a slit and passing through a prism; he placed a telescope about 24 feet away from the prism to observe the results (French. 2010).

Although many people believe that mid-infrared became popular before near-infrared, the fact is NIR was discovered prior to mid-infrared. While NIR spectroscopy and mid-infrared spectroscopy were both developed as instruments, NIR spectroscopy remained neglected for a long time by spectroscopists. Even though the NIR spectral region covered a wide range of absorption bands, the spectroscopists did not notice any interesting information in that spectral region, claiming that region presented broad, overlapped and weak absorption bands. In 1983, Wezel published paper entitled “Near-infrared Reflectance Analysis-Sleeper Among Spectroscopic Techniques" criticizing inconsiderate rejection of NIR (Pasquini, 2003).

Nevertheless, the real revolutionary time for NIR spectroscopy was in the 1980s. Between 1930 to 1980, 255 NIR applications were published, while the next ten years saw a marked increase in the number of applications (Pasquini, 2003). In the 1980s, spectroscopists directed considerable attention toward Near-infrared spectroscopy after performing many applications in industrial sectors and acquired more precise quantitative and/or qualitative results (Coates, 2006). As a result, more than 15000 publications on NIR technique was produced by 1998, which reveals a productive field for research using NIR technique (Pasquini, 2003).

Sampling is an issue for mid-infrared; however, it is considered to be advantage for near-infrared. Generally, the sample thickness is measured in the mid-infrared range from micrometers to tenths of millimeter, whilst in near-infrared no such issue arises when using greater thicknesses (millimeters or centimeters) to measure a similar quantum of light

absorption. Thus, near-infrared will be a suitable tool for sampling all phases of materials, particularly powdered or granular solids (Coates, 2006).

Theoretically, the general idea of near infrared is associated with the vibration of atom in a molecule. The NIR spectral region (12,000 -4000 cm^{-1}) mostly detects the following bonds present in any molecule (C-H, S-H, N-H, O-H) (Pasquini, 2003). The bands obtained from the NIR spectrum are based on vibration and combination. The vibration occurs when the radiation passes through the tested sample causing an excitation state to the molecule. Since the radiation is electromagnetic, it possesses energy that corresponds to a specific frequency. The molecular frequency should match with radiation frequency in order to obtain a signal in the spectrum. Carbonyl functional group in formaldehyde should be an adequate example. At room temperature, the bond between C and O in the carbonyl group (C=O) vibrates in a motion called stretching vibration. In reality the oxygen stretches and compresses as if there is a spring linked between the two atoms. In other cases, the carbonyl group moves back and forth in an oscillating motion. For each kind of vibration, there is a specific number of frequency matches with it. When measuring the frequency of formaldehyde, the radiation that passes through the sample will be absorbed and transmitted to the detector only if the light frequency matches up with the frequency of the molecule. Once the detector observes the transmitted light, the bands would show in the spectrum. Thus, the vibration process depends strongly on the characteristics of a bond wither it is single, double, or triple (EBSCO, 2011).

1.2 The basic principle of NIR

The fundamental theory of NIR spectroscopy aims to provide a clear picture of NIR absorption and the interaction between radiation and matter. The relationship between the radiation absorbed by a molecule and its vibration is simply described by Hooke's law (Burke, 1997).

$$V = \frac{1}{2}K(r - r_e) = \frac{1}{2}Kq^2 \quad (1.1)$$

Where: V is the potential energy. K is the force constant of the bond, r is the inter-nuclear distance during the vibration, r_e is the equilibrium inter-nuclear distance, and q is the displacement coordinate illustrated in Figure (1-2A) (Burns & Ciurczak, 2008). Along with potential energy, a model of a diatomic molecule was closely studied, and an equation of the vibrational frequency was derived:

$$\nu_0 = \frac{1}{2\pi}\sqrt{\frac{K}{m}} \quad (1.2)$$

Where the reduced mass m is given by:

$$m = \frac{m_1 m_2}{m_1 + m_2} \quad (1.3)$$

Based on those equations, the vibrational frequency is inversely proportional with mass of the molecule. In other words, the principle for investigating a chemical structure of a compound using infrared spectroscopy is based on the sensitivity of the vibrational frequency to the structure (Burns & Ciurczak, 2008).

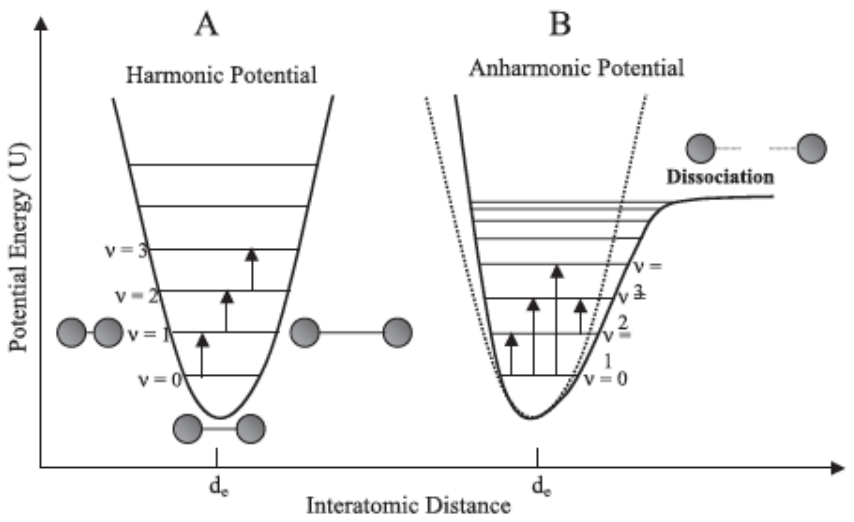

Figure 1-2: Schematic representation of the harmonic (A) and anharmonic (B) model for the potential energy of a diatomic molecule. de= equilibrium distance (U= minimum) (Pasquini, 2015).

1.2.1 The harmonic oscillator

The vibration of an atom can increase gradually if the atom absorbs energy. This model depicts an ideal behavior of the diatomic model; it assumes limited amplitude of vibration allows transition only between two adjacent levels when a photon is absorbed. From quantum theory, in NIR spectroscopy, the harmonic model fails in predicting the potential energy behavior of the molecular system since the system is characterized by having adjacent energy levels, and the absorbed energy can only permit transition by one energetic level (E_n). Accordingly, the vibrational energy will be calculated by the equation (Pasquini, 2003).

$$E_n = \left(n + \frac{1}{2}\right) h\nu_0 \qquad (1.4)$$

Figure 1-2A shows the transition between two adjacent energetic levels in the harmonic quantum model. These transitions are constant $\Delta\, \upsilon = \pm 1$. This means that the difference between two adjacent levels will be always the same. From here it is clear that the

harmonic model is able to simplify the principle of vibrational spectroscopy, it also limits the applications of NIR spectroscopy because the model refuses to allow transitions greater than $\Delta v = 1$(Pasquini, 2003).

1.2.2 The anharmonic oscillator

Anharmonic model is illustrated in Figure 1-2 B. It shows a better description of a diatomic molecule behavior. The model still depicted the molecule as two spheres for the atoms and a single bond connected them as a spring. However, the anharmonic/quantum model assumes a rapprochement between the two atoms and increasing in repulsion of the electrical charges surrounding the nuclei; lead to separation between atoms, which cause the bond force to change its behavior accompanied with rising in the potential energy. With high level of energy, over displacement is more likely to occur causing the molecule bond to rupture under the effect of the atomic nuclei.

By applying quantum mechanics, Remodelling Morse equation for the vibrational levels leads to the following equation.

$$E = h\nu\left(\upsilon + \frac{1}{2}\right) - x_m h\nu(\upsilon + \tfrac{1}{2})^2 \qquad (1.5)$$

In which x_m is the anharmonicity constant of the vibration, whose value is between 0.005 and 0.05.

Contrary to the harmonic model, the anharmonic/quantun model permits transition starts from v =2 or higher, and the existence of combination bands. Therefore, the combination and overtones bands are commonly observed in the NIR spectral region. (Pasquini, 2003).

1.3 Vibration modes

The interaction between the electromagnetic energy and a matter is mandatory in order to gain response in the NIR range, and without fulfilling this condition the absorption cannot occur. The active interaction occurs during the displacement that coincides with the excitation, leading to change in electric dipole moment of the molecule. Furthermore, The dipole moment is associated with the molecular vibration mode. For the basic model consisting of a diatomic molecule only one mode of stretching would correspond to its vibration motion. Taking into account other molecules have a number (N) of atoms, the vibration mode (stretching, wagging, bending, etc.) Figure 1-3 would be infrared active if it is asymmetric and has dipole moment, or infrared inactive if it is symmetric and absorb less light since there is no dipole moment (Figure 1-4) (Stuart, 2004).

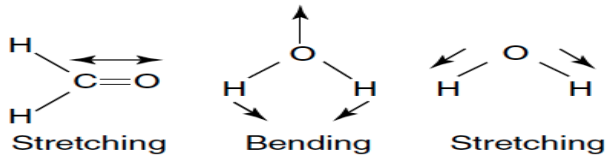

Figure 1-3: Stretching and bending vibration (Stuart, 2004).

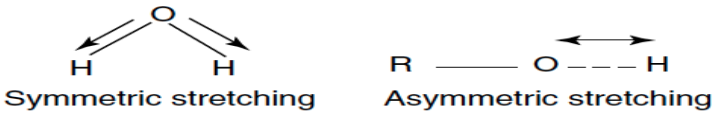

Figure 1-4: Symmetric and asymmetric vibration (Stuart, 2004).

Resonance occurs when a subject is exposed to an acoustic wave. For example, bowing a string in a violin would result in vibration only if the acoustic wave frequency and its natural frequency (physical characteristics) match each other. Thus, once the

string undergoes a high acoustic wave in open atmosphere the vibration energy would increase simultaneously. In the similar way, molecules can be excited to the vibrational level that matches up with a certain frequency of radiation. The overtones bands appear when the electromagnetic waves double the frequencies of the fundamental vibrations. For example, the fundamental vibration peak of carbonyl group in aldehyde is observed at 1720 cm^{-1} and the first and second overtone peaks would be at 3440, 5300 cm^{-1} (the fundamental vibration frequency is multiplied by 2 to calculate first overtone peak and is multiplied by 3 for second overtone band). However, the combination band is defined as the sum of fundamental vibration bonds located at different wavenumbers (v1+v2) (Kluger, 2011).

Resonance and coupling are two factors leading to misinterpretation of the NIR spectrum (Stuart, 2004). Primarily, Fermi Resonance occurs because of the similarity of the frequency of overtones or combination bands to the fundamental vibration frequency. Since the frequency is proportional to wavenumber, the resulting bands interfere, and the overtone wavenumber becomes closer to the wavenumber of the fundamental peak. This kind of overlapping makes the intensity of the fundamental peak weaker while overtone peak intensity is growing (Burns & Ciurczak, 2008). Secondly, coupling is more likely to happen if the molecule consists mostly of Carbon, Oxygen or Nitrogen. These bonds constitute the largest part of the vibration in the skeleton of the molecule. While each bond vibrates in a certain mode at different frequencies the vibrations become coupled. Hence the energy levels mingle and the spectrum would be full of bands that no longer referred to one bond. It was found that this phenomenon is ordinarily observed in the molecules that have these sorts of vibration modes "C–C stretching, C–O stretching, C–N

stretching, C–H rocking and C–H wagging motions."(Stuart, 2004). Three different amide compounds would be a good example demonstrating this phenomenon (Figure 1-5). Each one of the compounds has a distinct frequency assigned to the functional group in that molecule. The functional group vibrations influence the adjacent bonds to vibrate. As a result, the coupling vibration bands would be more likely to occur especially if the bonds have similar characteristic of strengths and reduced masses (Miller, 2011). Table 1-2 summarizes examples to demonstrate the absorption in NIR spectroscopy.

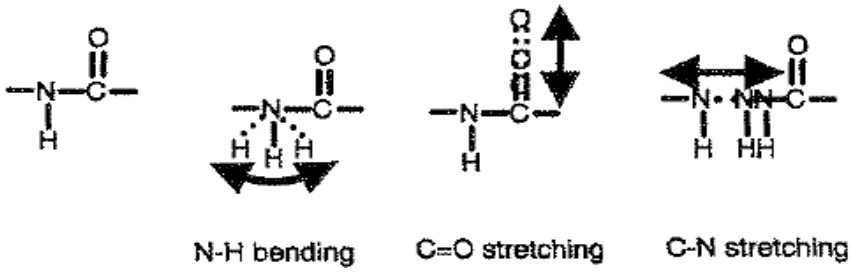

Figure 1-5: Coupled vibrations in the amide group (the "amide I" and " amide II" vibrations) In terms of individual functional group vibrations. " Amide III vibration (~ 1.650 cm-^{1}). ~80% C=O stretching; "amide II" vibration (~1.550 cm-^{1}): ~ 60% N-H bending and ~40% C-N stretching (Miller, 2011).

Table 1-2: Examples illustrate the active and inactive absorption.

Chemical bond example	Vibration mode	Absorption in NIR
Anharomic bond R-H (R= O, C, N)	Asymmetric stretch (has dipole moment)	NIR-active
Harmonic bond C=O	Symmetric stretch (no dipole moment)	NIR-inactive
H_2, O_2	Symmetric stretch (no dipole moment)	NIR-inactive

1.4 Summary and Thesis Overview

The purpose of this thesis is to provide an extensive literature review of NIR applications in diverse research areas. Particularly, focusing on characterizing the degree of deacetylation (DD) of chitosan. These objectives are clearly demonstrated in the second and third chapter. The second chapter is a review of NIR applications based on the most detectable bonds for this spectral region including O-H for water and alcoholic beverages, N-H in protein and other inorganic compounds, and C-H mostly found in all organic materials such as sugar. The applications were drawn from a large range of research areas to illustrate that the results follow the same pattern of analysis. Moreover, the regression methods, the NIR regions, and summary of reported application are demonstrated

The third chapter summarizes the experiment where the Degree of Deacetylation (DD) of chitosan is characterized using NIR. Verification of the experiment was preformed through demonstrating the DD of heterogeneous samples comparable to homogeneous samples that was used in previously. Results and discussion reveal successful calibration of chitosan in powder form.

2 Reviewed NIR applications

The purpose of this chapter is to review NIR applications based on the analyte and bond being determined, its wavenumber, processing method, and more importantly the concentration range with the standard error of calibration associated with each method being used. This chapter provides a review of the regression analysis methods commonly applied to FT-NIR spectra, the regions of NIR applicable to commonly reported applications, and the reported applications where the O-H, N-H and C-H bonds have been used to quantify concentration or chemical change in different industry sectors. The objective of this chapter is to provide a broader understanding of how NIR has been successfully employed, and the detection limits for this spectroscopic method of analysis.

2.1 Regression analysis

The penultimate step consists of the chemometrics software package. Chemometrics relies on extracting meaningful information from chemical data by analyzing these data using mathematics or statistics. The statistical techniques are multivariate analysis methods addressing the dominant patterns in the data and the relationship between two different parameters. Some of these techniques are Multi-linear regression, Principle component analysis, and Partial least square (Winefordner, 2004).

2.1.1 Multi-linear regression (MLR):

It is the oldest mathematical analysis method used to establish a linear equation that correlates two variables or more. To obtain this equation, several wavelengths need to be selected by one of the three modes: forward, backward, and stepwise (Roggo et al, 2007). The first mode is often better to apply on the first or second derivative spectra in

calibration equation; hence this regression delivers more accurate prediction by reducing poor fitted data (Clancy, 2010).

2.1.2 Partial least square (PLS):

Globally used in analysis of NIR spectra. The purpose of PLS is the ability to predict and estimate the relative link between two matrices. The variables on the x-axis represent the spectral data and the reference values are on the y-axis, where each value on the x matrix is best describing the data on the y matrix through eliminating the effect of the noise and baseline drift (Roggo, 2007).

2.1.3 Principal component analysis (PCA):

It is defined as an algorithmic approach used for classifying spectral data. PCA converts the variables set (correlated variables) into a coordinate set (uncorrelated variables). The number of the principal components corresponds to the linear combinations of x-variables. The first component has the maximum variation of all data, whereas the second component has less. The advantage of this technique is that there is no collinearity in the spectral data that can correlate the studied property and the computed principal components (Nørgaard et al, 2012)

2.2 Three NIR regions:

NIR has been applied widely in many different areas. Accordingly, dealing with multi-type samples might need special treatment or preparation. Therefore, The NIR region was divided into three regions; they were named based on the technique that is used in sampling and the measured material type where there is no need for prior preparation.

This advantage facilitates the use of NIR combined with other analysis tools such as UV-vis spectroscopy.

Reflectance region: 5405.41- 4000.00 cm^{-1} mostly suitable for measurement off ground and solid materials, which have rough surfaces. The incident light illuminates the surface sample at 0°. The surface reflects the light rays in different directions then the detector collects the light at a 45°. Combination bands occupy this region such as, C-H stretch and bend combination bands.

Transmission region: 8333.33- 5405.41 cm^{-1}. This analytical technique is used in UV-vis, Mid IR, and Atomic absorption. The transmitted light, passed through a transparent sample (clear liquid or film), is measured by detector whereas the chemical components absorb some of the energy. Therefore, the region is applied to analysis of water, metals, biological and organic materials. The 1st and 2nd overtones of the fundamental stretch bonds in the Mid IR region exhibit the absorption bands.

Transflectance region: 13888.89- 9090.91 cm^{-1}. The name of this technique is a combination of two analytical methods (reflectance and transmission). Thick samples are analyzed by transmitting and reflecting the light from the surface sample simultaneously. The sample could be seeds, pastes, slurries, and liquids. The 3rd overtone bands exhibit the absorption the fundamental stretch bonds in the Mid IR region (Martin, 2008).

2.3 Functional groups and bonds:

2.3.1 Hydroxyl group (OH):

It is as a distinct sign of alcohols, and can be found in a variety of organic and inorganic compounds. Due to the response of polar bonds to NIR light, many of these compounds have reference bands in the NIR region (4000 to 12.500 cm^{-1}). O-H is a polar functional group possessing a permanent dipole moment, which leads to incitement of vibrational bands. In the case of water, H_2O is a triatomic nonlinear molecular with three vibration modes: symmetric stretch with a band at 7370 cm^{-1}; asymmetric stretch at 7012 cm^{-1}, and scissoring bend at 11310 cm^{-1} (Standard, 2015). These two conditions enhance absorption of a molecular thus water bands appear clearly in the three sections of NIR spectral regions (transflectance, transmission and reflectance). Generally, all OH groups have strong bands in the third region (4000 to 6000 cm^{-1}). The absorbance of NIR light by OH group is affected strongly by temperature, and must be corrected for during analysis (Burns & Ciurczak, 2008).

Moisture: NIR is highly responsive to the water bond O-H; thus, the measurement of moisture is an uncomplicated process. Water absorption in the NIR region exhibits three bands and the most obvious one is found in the region of 5300-5150 cm^{-1}. Table 2-1 provides a summary of 11 recently reported applications on the use of NIR to determine moisture and alcohol content.

NIR is able to monitor water concentrations over a broad range, from several wt% to ppm levels in a liquid sample. For liquid samples, the moisture contents reported ranged from 13 ppm to 650 mg/g. In most applications reviewed, the SEC was approximately 0.02 to

0.04 wt%, but did go as high as 37.88 mg/g, and as low as 4ppm depending on sample quality and purity (Table 2-1).

Alcohol: The O-H bond is used to determine alcohol content as well. NIR is extensively applied in the characterization of a variety of alcoholic beverages due to the absorption of O-H in the fourth and third overtone region (13500-13800 cm^{-1}), second region (11800-11500 cm^{-1}), first region (7000-7300 cm^{-1}), and combination bands region (4850- 4950 cm^{-1}). It should be noted that H_2O bands appear at similar wavenumbers with greater intensity than the O-H band, so peak interference may be a challenge when determining O-H bonds in an aqueous solution. One of the most successful calibrations was able to determine alcohol content from 2.9% to 4.84% with a root mean square error of calibration (RMSEC) of 0.0435% (Table 2-2).

Table 2-1: Summary applications of NIR to quantify water (O-H).

Application Tittle	Chemicals/ parameters	Functional group	Wave# range	Post-processing method	Approximate concentration range	Reference
Monitoring water, methyl acetate, and methanol	Water. Methyl acetate, methanol.	O-H, C-H	5208.33 cm^{-1} for Water. 5973.72 cm^{-1} fro methyl acetate. 4793.86 cm^{-1} for methanol.	Path length 1 mm is used	Water concentration ranging from 0–5%, methyl acetate concentration from 0–49%, and methanol from 49.7–99.7%. The SEC is 0.8%.	(Application Bulletin 409, 2013).
Monitoring moisture in ethylene glycol samples	Ethylene glycol	O-H	5102.04 cm^{-1}	2 mm path length cuvette.	The samples concentration from 0–5%. The SEC is 0.1%	(Application Bulletin 409, 2013).
Near infrared spectroscopy (NIRS) for on-line determination of quality parameters in intact olives	Acidity, moisture and fat content in intact olive fruits	O-H, C-H	10309.28 cm^{-1} and around 8333.33 cm^{-1} O-H stretching vibration & C-H second overtone. 6944.44 cm^{-1} for O-H stretching first overtone	Raw spectra, PLS, PCA	The content range Acidity 0.09-26.06 Moisture 31.42-74.55 Fat 5.11-30.34 residual predictive deviation (RPD) Acidity 1.63 Moisture 0.98 Fat 1.08	(Salguero-Chaparro, el at, 2013).
Feasibility of near-infrared spectroscopy to predict aw and moisture and NaCl contents of fermented pork sausages	Water activity (aw), moisture, and NaCl contents in fermented pork sausages	O-H, C-H groups	5153 cm^{-1} and 6800–7000 cm^{-1} for O-H stretching.5800–5675 cm^{-1} and around 8277 cm^{-1} for C-H_2 and C-H	1st Derivative, PLS	The (RPD) Moisture (%) 19.8- 21.6 aw 9.22 - 8.26 NaCl (%) 6.91 -6.23	(Collell, and el at, 2010).
Analysis of water in food by near infrared spectroscopy	Water content in different samples	O-H	7407.41 –5882.35 cm^{-1} region from 2nd Derivative.	Raw spectra, 2nd Derivative, PCA	The fermented samples (70%-24.1%). cottage cheese fall within 0.25%.	(BuÅNning-Pfaue, 2003).
Monitoring parts-per-million (PPM) levels of moisture in phenol	H_2O	O-H	5230.13 cm^{-1}	PLS, 10 mm path length	The concentration of moisture ranging from 170–10,000 ppm. And SEC of 36 ppm.	(Application Bulletin 409, 2013).
Application of near-infrared spectroscopy for moisture-based sorting of green hem-fir timber	Moisture in timber	OH, CH	6993.01 cm–1,5235.60 cm–1 for OH.7336.76 cm–1, 7215.01 cm–1 for CH in Cellulose.	Raw spectra, partial least square PLS,	Moisture content of the samples ranged from 35% to 105%. And root mean square error of prediction (RMSEP) of 5.70%.	(Watanabe, Mansfield, Avramidis, 2011)
Monitoring water, chloroform, carbon tetrachloride, dibromobenzene, chlorine, sulfate and oil in a bromine liquid	Water Chloroform Oil	O-H, C-H	5208.33 cm^{-1}, 4436.56 cm^{-1}, 4533.09 cm^{-1}	20 mm path length cuvette	The concentration of H_2O (13–55 ppm), and SEC of 4 ppm, the concertation range of CCL_4 (13–36 ppm), (SEC of 4 ppm), the oil concentration range from (0.1–0.23 ppm) and SEC of 0.03 ppm.	(Application Bulletin 409, 2013).

Table 2-2: Summary of NIR application to quantify alcohol content.

Application Tittle	Chemicals/ parameters	Functional group	Wave# range	Post-processing method	Approximate concentration range	Reference
FT-NIR Analysis of Czech Republic Beer: A Qualitative and Quantitative Approach	Alcohol content	O-H	Qualitative region 10,000 to 5400, Quantities region 10,000–5400 cm^{-1} 4700–4100 $cm^{-1.}$	2 mm transmission cell. Raw spectra, 2nd Derivative, PLS	Alcohol content ranged from 2.9% to 4.84% with RMSEC of 0.0435	(Budinova, Dominak, and Strother, 2008).
FT-NIR Analysis of Wine	Ethanol	O-H	4400 cm^{-1}.	1 mm glass cuvettes, 2nd Derivative, PLS	Concentration range (4.23 and 27.63) RMSEC of 0.23	(Hirsch, 2013).
Acid and Alcohol NIR Analysis as Examples of Food Process Control	Alcohol content	O-H	Two regions were used 5100 to 4800 cm^{-1} and 7700 to 5400 cm^{-1}.	Raw spectra.	The alcohol content ranged from 0.28% to 3.47%. RMSEC of 0.0768	(Thermoscientific, 2013).
NIR spectroscopy and fibre optic probe for determination of alcohol, sugar, tartaric acid in alcoholic beverages	Alcohol content	O-H	4000-7000 cm^{-1}	Path length 0.2-20 mm, Raw spectra, PCA	Alcohol content ranged from 10 % to 20% with standard error of prediction RMSD 0.4831	(Mehrotra, Gupta, and Nagarajan, 2005).

2.3.2 Amine group (N-H):

The three types of amine (Primary, Secondary, Tertiary) are available in abundance in foods and agricultural products. In industry, NIR has gained prominence as a precise analytical technique in determining the quality and quantity of products by detecting N-H bonds. The NIR regions that N-H bonds occupy are 3rd overtone (1300-11000cm^{-1}), 2nd overtone (10000-9000 cm^{-1}), 1st overtone (6800-6500cm^{-1}), and the combination bands region (4850-4550 cm^{-1}). In reviewing 13 recent reported applications (Table 2-3), NIR has been able to determine N-H linked compositions with standard errors ranging from 0.02 to 0.4% over a range of 0 to 70% amine content. In addition, the response of nitrogen-containing compounds has been used to quantify inorganic compounds such as sodium azide (N=N) to an accuracy of 0.3 to 2% for compositions ranging from 1 to 75%.

Proteins are an important constituent in a variety of products; therefore, most of NIR applications focused on determining different types of proteins. Since the chemical structure of proteins is composed of the three of the most detectable bonds N-H, O-H, C-H, the NIR calibration is quite accurate. After reviewing a number of applications (Table 2-4), NIR is capable to predict the protein content ranging from 2.65-86% with a SEC of 0.08 - 3%.

Table 2-3: Summary of NIR application to quantify the content of amine (N-H).

Application Tittle	Chemicals/ parameters	Functional group	Wave# range	Post-processing method	Approximate concentration range	Reference
Monitoring the primary amine present in a treated clay	Primary Amine	RNH	4940.71 cm^{-1}, 6510.42 cm^{-1}	Unknown	The concentration of amine samples ranges from 0.7–2.3%. SEC of 0.1%.	(Application Bulletin 409, 2013).
Monitoring primary and tertiary amines in clay samples	Tertiary amine Primary Amine Mixture of tertiary and primary amines	R3N RNH R3N+RNH	4868.55 cm^{-1}, 4940.71 cm^{-1}, 4405.29 cm^{-1}	Unknown	The content of tertiary amine (0.2–1.0%), SEC of 0.02%. the content of primary amine (0.7–2.3%). SEC of 0.1%. For the samples treated with both tertiary and primary amines (0.2–1.0%). SEC of 0.04%.	(Application Bulletin 409, 2013).
Monitoring quaternary amine in clay samples	Quaternary amine	NR4	6142.51 cm^{-1} 6024.10 cm^{-1}	Unknown	The range of quaternary amine is (0–8%). SEC of 0.02%.	(Application Bulletin 409, 2013).
Monitoring a process stream of diethylaniline (DEA) and diethylphenyl azomethine (AZO)	Diethylaniline (DEA)	C-N	9784.74 cm^{-1}	20 mm path length	The concentration ranges of DEA from 5–80%. And SEC 0.6 %	(Application Bulletin 409, 2013).
Monitoring the presence of ammonia in vinyl pyrrolidone	Ammonia NH3	N=H	6561.68 cm^{-1}	A 10 mm quartz cuvette.	The ammonia concentration range (0–100 ppm). With SEC of 14.0 ppm	(Application Bulletin 409, 2013).
Monitoring the concentration of sodium azide in an airbag formulation	Sodium azide Sodium nitrate	N=N N=O	7429.42 cm^{-1}, 4734.85 cm^{-1} 6119.95 cm^{-1}	Unknown	Sodium azide concentration ranging from 66.23–74.27% (W/W). SEC of 1%. nitrate concentration was 2.9–6.4%. SEC 0.7%.	(Application Bulletin 409, 2013).
Determination of total volatile basic nitrogen (TVB-N) content and Warner–Bratzler shear force (WBSF) in pork using Fourier transform near infrared (FT-NIR) spectroscopy	Ammonia (NH3), trimethylamine (TMA) and dimethylamine (DMA),	N-H groups, C-H3	5638.8–5368.9, 8921.1–8655.0 and 9191.1–8924.9 cm^{-1}	Raw spectra, Synergy interval partial least square (SI-PLS) algorithm	The PLS model of TVB-N content was achieved with Rc = 0.7242, RMSECV = 4.2 mg/100 g in the calibration set, and Rp = 0.6780, RMSEP = 4.80 mg/100 g in the prediction set.	(Cai, Chen, Wan, and Zhao, 2010).
Quantitating phenylalanine and water in L-phenylalanine cake samples.	Phenylalanine	CONHR	4803.07 cm^{-1}	Unknown	The content of phenylalanine range from 65.84–74.9%. (SEC of 2%).	(Application Bulletin 409, 2013).

Table 2-4: Summary of NIR applications to quantify protein content (N-H).

Application Tittle	Chemicals/ parameters	Functional group	Wave# range	Post-processing method	Approximate concentration range	Reference
Determination of Protein Content by NIR Spectroscopy in Protein Powder Mix Products	Protein	C-H, N-H.	8928.57 -7407.41 cm^{-1}, 6250.00 -5405.41 cm^{-1}	Raw spectra. 2nd Derivative, PLS	Protein content range from (8.7-86)% with SEC of 3%.	(Ingle, and et al, 2016).
Influence of feed source on determination of fat and protein in milk by near-infrared spectroscopy	Protein and fat content in milk	C=O, N-H, O-H, C-H,	5820.72 &4329.00 cm^{-1} Correspond to fat 6587.62, 4604.05, 4492.36 &5720.82 cm^{-1} Correspond to Protein	Raw spectra, PLS, MLR	The RPD Fat (0.85-7.40) SEC of (0.25) Protein (2.65-3.91) SEC of (0.08)	(Purnomoadi, Batajoo, Ueda, and Terada, 1999).
Measurement of the protein composition of single wheat Kernels using near infrared spectroscopy	Protein	N-H	50000.00 -40000.00 cm^{-1}	Raw spectra, PC.	Protein low content in different sample range 0.0-36.9% and high content 0.9-45.6% with RMSEC range from 0.14-3.59%	(Wesley, Osborne, Larroque and Bekes, 2008).
Protein, Fat and Moisture Analyses of Fresh Fishmeal with an Antaris II FT-NIR Analyzer	Protein, Fat, water, ash, NH3	N-H, OH, C=O.C-H	9000-400 cm-1	Raw spectra, first derivative with a Norris smoothing of length= 3 and a gap = 3, PLS	Protein (68.7-72.3) RMSEC of 0.57 Fat (8.3-10.5). RMSEC of 0.27 NH3(0.12-0.25).RMSEC of 0.012 Ash (12-15.67). RMSEC of 0.605 Water (5.6-9.3).RMSEC of 0.242	(Wiertz, 2010).
Determination of protein, total carbohydrates and crude fat contents of foxtail millet using effective wavelengths in NIR spectroscopy	Protein, Fat, Carbohydrates	C–H, O–H and N–H	8849.56, 8097.17, 7194.24, 6514.66 cm-1	Raw spectra, MLR, PLS.	Protein content range (g/100g) 9.5- 18.9 with SD of ± 2.2. Total carbohydrates range 71.5- 83.8 with SD of± 2.6. Crude fat content range 4.4-7.3 with SD of ± 0.7.	(Chen, Ren, Zhang, Diao, and Shen, 2013).

2.3.3 C-H Bonds:

It is the primary component of organic compounds found in nature. Four bonds, predominantly covalent bonds, surround carbon. It can be one bond between two carbon atoms or two to three bonds between two carbons. In chemistry, hydrocarbon compounds were classified as alkanes, alkenes, alkynes, and aromatic hydrocarbons. Each bond that belongs to a specific group has different intense absorption band based on the polarity of the analyte sample. C-H bands can be observed in 4th overtone (14000-12800 cm^{-1}), 3rd overtone (12000-10500 cm^{-1}), 2nd overtone (9100-8500 cm^{-1}), 1st overtone combinations (7500-6800 cm^{-1}), combination bands region (4500-4000 cm^{-1}).

Sugar contains C-H bond as well as other bonds such as O-H, C=O. Fructose, sucrose, glucose are three forms of sugar that have received great attention of NIR researchers. In the food industry, the quantity of sugar needs to be identified as a part of the nutritional value label; therefore, NIR has been used frequently in fruit juice, honey, and syrup. Recently, 5 reported applications illustrated in Table 2-5 elucidate NIR ability to predict the concentration of all of the three sugar forms at low level, 1.21% for glucose, 0.06% for sucrose, and 0.13% for fructose with SEC of $\pm$0.0194%. The most successful calibration for high level of sugar forms is 86.4% $\pm$0.163% for fructose, 35.18% with SEC of $\pm$0.197 for glucose, and 15.02(% w/w) With SEC of $\pm$0.04% for sucrose.

Table 2-5: Summary of NIR applications to determine sugars content (C-H).

Application Tittle	Chemicals/ parameters	Functional group	Wave# range	Post-processing method	Approximate concentration range	Reference
NIR detection of honey adulteration reveals differences in water spectral pattern	High fructose corn syrup (HFCS) mixed with four artisanal Robinia honeys at various ratios (0–40%)	O-H & C-H groups	7374.63 cm^{-1}, 6973.50 – 6963.79 cm^{-1}, 6775.07 cm^{-1}, 6657.79 cm^{-1}, and 6329.11 cm^{-1} for OH & 5917.16 cm^{-1}, 5787.04 – 5780.35 cm^{-1}, and 5617.98 cm^{-1}, are for C–H stretching	Raw and 2nd Derivative. PLS, PCA.PCR.	Pure honey samples and HFCS 87.2 ± 0.65 (mean ± SD) & 81.3 %. Mixture samples 86.4 ± 0.71 (mean ± SD). Standard error of laboratory (SEL) for the reference measurement was 0.11.	(Bázár, and et al, 2016).
Rapid analysis of sugars in fruit juices by FT-NIR	Aqueous solutions of sugar mixtures (glucose, fructose, and sucrose).	O-H, C-H groups	A. Transmittance (7500-7000, 6000-5400, 4700-4000 cm^{-1}. Transflectance(7300-6700, 6000-5400, 4800-4150 cm^{-1}).	2nd Derivative, PLS	Apple Juice (g/100 mL) Sucrose Glucose Fructose (1.11-2.74) (2.45-3.26) (6.42-7.79) Orange Juice (g/100 ml) Sucrose Glucose Fructose (3.82-4.59) (2.14-3.02) (2.81-3.05)	(Rodriguez-Saona, et al, 2001).
A feasibility study on quantitative analysis of glucose and fructose in lotus root powder by FT-NIR spectroscopy and chemometrics	Glucose Fructose	C-H, C=O	4000,6060,8000, 12,432, and 4545 cm^{-1}	Raw spectra, partial least-squares regression (PLSR), interval PLS of forward (FiPLS) and backward (BiPLS),	Glucose 31.12–34.86 With RMSEC of 0.035-1.23. Fructose range from 0.76 to 1.78 %, with RMSEC of 0.061-0.449.	(Xiaoying, Zhilei, Kejun, Xiaoting, 2012).
Determination of origin and sugars of citrus fruits using genetic algorithm, correspondence analysis and partial least square combined with fibre optic NIR spectroscopy	Sucrose, glucose and fructose.	O-H, C-H	6896.55, and 5154.64 cm^{-1} correspond to O-H. 7132.67 and 7342.14 – 7204.61cm^{-1} first overtones of O-H and C-H 5952.38 – 5701.25 cm^{-1} assigned to first overtones of C-H stretching	Raw spectra. PLS.	The range of prediction concentration by NIR. Sucrose (0.06-1.85), Glucose (1.21-2.98), Fructose (0.13-1.5). And SEC of 0.0194	(Tewari, and et al, 2008).
Determining sucrose and glucose levels in dual-purpose sorghum stalks by Fourier transform near infrared (FT-NIR) spectroscopy	Sucrose, glucose	C-H group, O-H	6930–6944 cm^{-1} O-H stretch 1st overtone, 4295 C-H stretch/ C-H deformation combination, 4403–4405 cm^{-1} O-H stretch/C=O stretch combination, 5186 cm^{-1} O-H combination.	Raw spectra, PLS	Sucrose contents ranging from 0.52 to 15.02% (w/w) with SEC of 0.197 and glucose contents ranging from 0.29 to 6.88% (w/w) and SEC of 0.04.	(Chen, and et al, 2014).

Moreover, recent reported publication (Phan-Thien et al, 2011) shows that NIR spectroscopy can be used to determine the concentration level of minerals such as (Mg, K, CL, and P). In addition, NIR spectroscopy extensively used in industry for quantitative and qualitative purposes as shown in Table 2-6. For example, the desired quality could be hardness or potential for damage caused by high or low concentration level of moisture in fruits.

Table 2-6: Summary of NIR applications used quantitatively and qualitatively.

Application Tittle	Chemicals/ parameters	Functional group	Wave# range	Post-processing method	Approximate concentration range	Reference
Starch Waxiness in Hexaploid Wheat (Triticum aestivum L.) By NIR Reflectance Spectroscopy	Testing the waxy condition	N-H groups	4370.63- 4325.26 cm^{-1}.	Raw spectra, 1st Derivative, 2nd Derivative, PCA.	Protein content range from13.6-14.2%, and SE range from 1-1.6. Amylose fraction in isolated starch content range from 0.8-25.5 %, and SE grange 0.83-3%. Single-kernel mass (mg) range from 36.6 to 37, and SE range from 5.9-6.8.	(Delwiche, Graybosch, Amand, and Bai, 2011).
Rapid quantification of flavonoids in propolis and previous study for classification of propolis from different origins by using near infrared spectroscopy.	Flavonoids	C-H groups, O-H	5780.35- 5000.00, 4545.45- 4166.67, 9090.91- 6250.00 cm^{-1}.	Raw spectra, 1st Derivative, PCA.	The content of flavonoids (g/g) range from 0.002- 21.02, and RMSECV (g/g) range from 0.0213- 0.132	(Cai, Wang, Meng, Meng, and Zhao, 2012).
Near-infrared spectroscopy for medical applications: Current status and future perspectives.	Triglycerides	C-H groups, C=O.	16666.67- 9090.91 $cm^{-1.}$	Raw spectra, PLS	Triglycerides concentration 38–572 mg/dL, and 43.68 mg/dl.	(Sakudo, 2016).
NIR Spectroscopy Applications for Internal and External Quality Analysis of Citrus Fruit—A Review.	Defecting, canker, green mould.	C-H groups, O-H.	14,800–5,200, 6,950–7,100, 4,720–5,400, 8,100–9,100 cm^{-1}	Raw spectra, PCA, PLS. MLR	The good quality of fruits is described by RMSEC, RMSECV and RMSEP range. Some of the parameters addressed have RMSEC range from 0.1-5, others have RMSEP range from 0.013- 66.78, and SEP range from 0.018- 6.054.	(Magwaza, et al, 2011).
NIR Spectroscopy Applications in the Development of a Compacted Multiparticulate System for Modified Release	Compression force, crushing force, and content uniformity of Theophylline tablets and Crushing force, and Compression force of Cimetidine tablets.	O-H peaks have great intensity	5175.98 cm^{-1}, Other wavenumbers of peaks were consider 6009.62 cm^{-1}, 4578.75 cm^{-1}, 8431.70 cm^{-1}, 5889.28 cm^{-1}.	2nd Derivative, PCA, PLS.	Dataset is considered (40–350 kg) for compression force with SEC of 30.99Kg for Theophylline and 24.85 Kg for Cimetidine. For the Crushing Force of Theophylline content (15-17.1) mg, and Cimetidine content (15-17.1) mg the SEC is 0.47, and 0.35mg respectively. For content uniformity, both tablet content range from 10.5 to 19.5 mg. with SEC of 0.31 of theophylline, and 0.47 mg for Cimetidine.	(Cantor, el at, 2011).
Assessment of resin formulations and determination of the formaldehyde to urea molar ratio by near- and mid-infrared spectroscopy and multivariate data analysis	The molar ratios of formaldehyde (F) to urea (U) of three resin formulations	N-H, and C-H groups	NH bending at 5080–4980 cm^{-1}, C-H_2, C-H at 4315 $cm^{-1.}$	1st Derivative, and 2nd Derivative, path length is 1 mm, PCA, PLS.	The formaldehyde to urea molar ratio rang from 0.9 to 1.49 The RMSECV rang from 0.005 to 0.007.	(Costa, el at, 2013).

Application Tittle	Chemicals/ parameters	Functional group	Wave# range	Post-processing method	Approximate concentration range	Reference
Classification of maize kernel hardness using near infrared hyperspectral imaging	Hardness	C=O, C-H, O-H, N-H.	7087.17, 5194.81, 4807.69, 7315.29, 5065.86, 6872.85cm^{-1}	Digital images and PCA images	Vitreous endosperm (%) hardness range from 47- 73, intermediate 49-71, soft 47-63, and the SD range from 4-5. Floury endosperm (%) hardness range from 5-36, intermediate 8- 27, soft 13-29, with SD range from 4-5. germ and pericarp (%) hardness range from 17-34, intermediate 15-29, soft 21-29, and the SD range 2-3.	(Mcgoverin, and Manaley, 2012).
FT-NIR spectroscopy as a tool for valorization of spent coffee grounds: Application to assessment of antioxidant properties	2,2′-Azino-bis (3-ethylbenzothiazoline-6-sulfonic acid) diammonium salt (ABTS)	O-H	Region 1 (5000–4000 cm^{-1}), region 2 (6700–5350 cm−1), region 3 (10,000–7300 cm^{-1}), region 4 (5350–5000 cm^{-1}) and region 5 (7300–6700 cm^{-1}).	Raw spectra, PLS	The coffee volume ranges 10-100 ml. The range error ratio (RER) for the region from (6700-5350 cm^{-1}) is 13.5-18.3.	(Lopes, 2013).
Application of LS-SVM to non-linear phenomena in NIR spectroscopy: development of a robust and portable sensor for acidity prediction in grapes	The acidity of three different grape varieties	C=O. O-H	14705.88 –9090.91 cm^{-1}	MLR, PLSR.	LS-SVMl has the lowest value of The Standard Error of Prediction (SEP) 1.03	(Chauchard, Cogdill, Roussel, Roger, Bellon-Maurel, 2004).
NIR analysis of cellulose and lactose—Application to ecstasy tablet analysis	Lactose in different chemical forms.	O-H, C-H groups, N-H.	9090.91 cm^{-1} - 4000.00 cm^{-1}	Raw spectra, PLS.PCA	The purity of samples is (5-10-15) with SEC 0.2%. The samples mixed with excipient range from 1-4% with SEC 0%.	(Baer, Gurny, and Margot, 2007).
Determination of persimmon leaf chloride contents using near-infrared spectroscopy (NIRS)	Chloride content	N-H, O-H	6548.79 cm^{-1}, 6397.95 cm^{-1}, 5012.53 cm^{-1}, 4782.40 cm^{-1}	1st Derivative, PLS, PCA.	The chloride contents ranging from 0.76 to 1.78 %, with SEC 0.007%.	(Paz, Visconti, Chiaravalle, and Quiñones, 2016).
Feasibility of estimating peanut essential minerals by near infrared reflectance spectroscopy	Minerals compositions	K, P, Mg, Ca	4215.85 - 8849.56 cm^{-1}, 8025.68 - 5753.74 cm^{-1}, 7142.86 - 6451.61- 5405.41 - 4545.45 cm^{-1}.	2nd Derivative, PLS	The content of Ca: in set A (605 ± 136), set B (598 ± 110), with RMSEC of 108.2602. For K, Set A (7056 ± 793), set B (7452 ± 878), and RMSEC ranged from (48.993-369.283). For Mg, Set A (1678 ± 192), set B (1766 ± 197), and RMSEC ranged from (73.033- 541.053). For P, Set A (4556 ± 1200), set B (3940 ± 466), and RMSEC of (238.243)	(Phan-Thien et al, 2011).

2.4 Summary

This chapter has reviewed a number of recent publications on the use of NIR for quantitative analysis in literature. NIR appears to be a useful tool for the characterization of moisture, alcohol content, amine bonds and structural changes, which modify C-H, and related bonds. This method of analysis also benefits from a greater penetration depth during analysis, reducing the sample preparation requirements relative to IR-based methods. Overall, due to the high sensitivity of NIR spectroscopy to water, O-H band is used to assign monitoring the content of water or moisture in many different products. The recent reported applications show successful calibration up to 4 ppm. Other bonds of interest are found in the most of investigating sample are N-H, and C-H. The content of protein and sugar is determined by NIR spectroscopy through analysis bonds referring to N-H, and C-H. The SEC of sugar ranges from 0.0149 to 0.197, and the SEC of protein ranges from 0.08 - 3%.

One significant benefit of this is that NIR is highly suitable to characterizing solids. To demonstrate this, Chapter 3 focuses on a challenging characterization problem: determination of the degree of deacetylation of chitosan particles without dissolving them in a solvent (i.e. raw powder analysis).

3 Determination of the Degree of Deacetylation of Chitosan

Chitosan, (1,4)-[2 amino-2-deoxy-¯-D-glucan, is a bio derived polymer obtained from marine animals such as shells of crustaceans, jellyfish or corals (Biniaś and Biniaś, 2014) as shown in Figure 3-1. Chitosan can be obtained from chitin through a deacetylation process, defined as the chemical process of removing acetyl groups from chitin molecule. The degree of deacetylation is the percentage of free amino groups found in chitosan molecule (Momin, 2008).

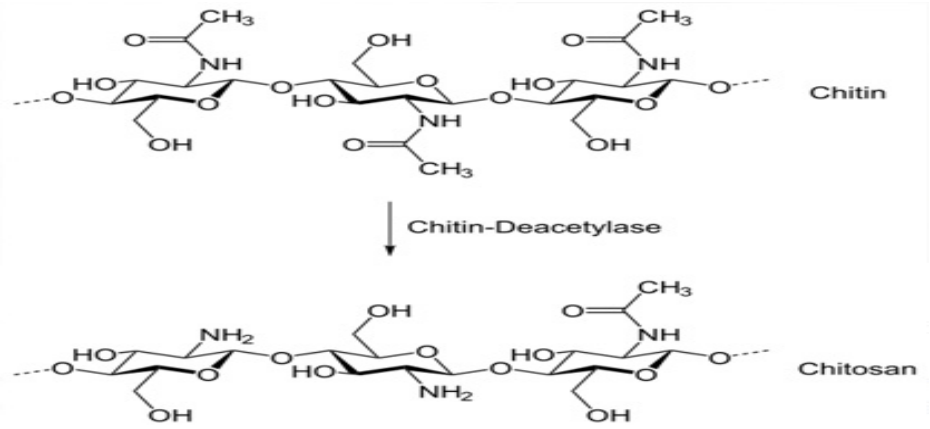

Figure 3-1: Chemical structure of chitosan.

The degree of deacetylation is vital and it is one of most important characteristics that can affect the properties of chitosan and its applications. Two degrees of deacetylation were explored with a drug called 5-FU, an anti-neoplastic agent used extensively in clinical chemotherapy for treatment of solid tumors, e.g., bowel, breast, stomach, and pancreas cancers" (Yang and Hon, 2010). Unfortunately, 5-FU has negative impact on the human body cells, that eventually leads to serious side effects such as hair loss, birth defects, mouth sores. Chitosan was proposed to be used with the drug in order to alleviate some of the said effects, with the result showing the release of 5-FU was faster with combination of chitosan having DD= 90% compared to DD=75% (Figure 3-2, Yang and Hon, 2010). Higher DD corresponds to more free amino groups

present in the molecule that facilitate the solubility in the solvents. For this oral drug, the solvent would be stomach acid, which is has low PH very suitable to dissolve a weak alkaline compound (Kumirska et al, 2011).

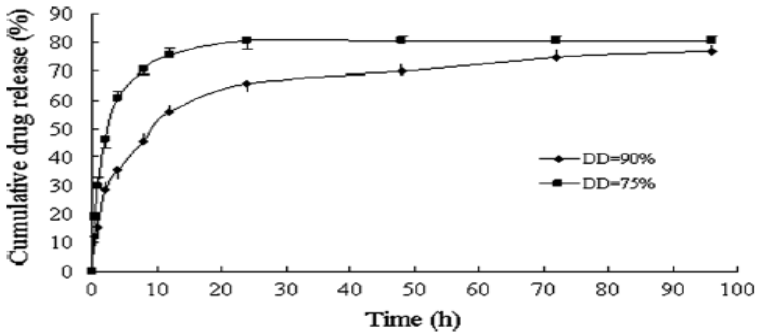

Figure 3-2: In vitro release profiles of 5-FU from chitosan nanoparticles in PBS solution

Currently the DD of chitosan powders is determined through a number of experimental methods. These include acid-base titration (Li et al, 2012), potentiometer titration (Yuan et al, 2011), and ultraviolet-vis spectroscopy (Yuan et al, 2011). In acid-base titration, chitosan is dissolved in HCl and titrated using NaOH where the amount of HCl and NaOH added for given mass is used to determine the free amino content. From this, the DD can be determined. In potentiometer titration, chitosan is dissolved in HCl and titrated using NaOH, where the inflection points of the pH curve during NaOH addition allows the percentage of free amino groups to be determined. In existing spectrophotometeric methods, the absorbance of chitosan at 199 nm was found to correlate well with the presence of acetyl groups. Using N-acetylglucosamine as a standard of fully acetylated functional group, the DD can be calculated by determining acetyl groups concentration measured relative to the total concentration of chitosan in solution. This method still requires dissolution of the chitosan prior to characterization.

The aim of this study was the development and validation of NIR-based methods for determining the DD of chitosan without the need of solvents.

3.1 Methodology:

The degree of deacetylation was measured for four Chitosan powders of known DD (80%, 96.1%, 98.4%, and 100%). For each sample, a small amount was placed in a flat-bottomed glass vial of approximate diameter of 2 cm. The spectra of each sample was then collected using the diffuse integrating sphere module on the Antaris-II FTNIR, with background samples collected each day to account for changes in atmospheric conditions within the lab. For each powder sample, multiple spectra were obtained for centered and off-center vial placement to explore the impact of measurement error, as well as for different powder quantities to define minimum sample sizes required for characterization (Table 3-1).

Table 3-1: Example of spectral measurements preformed for 98.4% of chitosan.

Cap On/Off	Vial position	Mass	Sample
On	Center	0.2794	1
Off	Center	0.2794	1
On	Edge	0.2794	1
On	Center	0.2794	2
On	Center	0.2794	3
On	Center	0.5455	1
On	Center	0.5455	2
On	Center	0.5455	3
On	Center	0.8058	1
On	Center	0.8058	2
On	Center	0.8058	3

3.2 Results & Discussion:

The full spectra of the samples analyzed are shown in Figure 3-3 for the four DD tested. Through analysis of these spectra, it was determined that the sample placement (edge vs. centered) and mass of powder used in these studies had minimal effect on the spectra measured

for a given DD. This would indicate that while care should be taken in preparing and placing sample vials on the detector, it is tolerant to variations in vial placement and variations in the quantity of powder in the sample vial. During deacetylation; the significant change in the molecular structure of chitosan is the conversion of an R-NH-R bond into R-NH_2, and the loss of an acetyl group (N-$COCH_3$). Given this change in structure, the suggested regions of interest within the NIR spectra correspond to the R-NH_2 overtone region and the organic regions. Since the DD is a ratio of D-glucosamine units per 100 monomers expressed as a percentage, the -CH_2- bond is included. Within the near infrared range, the organic overtones appear at wavenumbers between 5962-5719cm^{-1} as shown in Figure 3-4. The characteristic oscillation for the first overtone of the N-H band is shown in Figure 3-5 for a subset of the powders tested. Through analysis of the spectra obtained, a strong correlation was observed between the raw spectra in the two regions illustrated in Figures 3-4 and 3-5 and the DD.

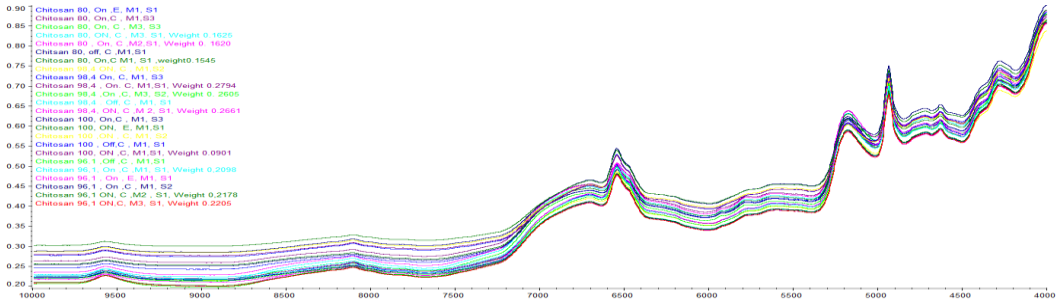

Figure 3-3: NIR raw spectra.

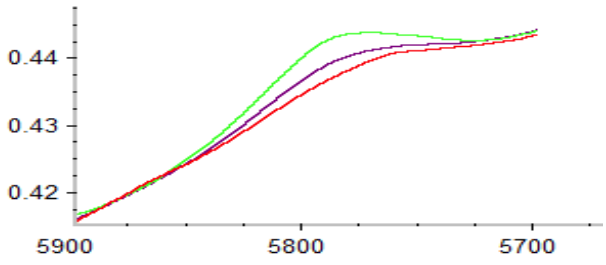

Figure 3-4: C-H (1st overtone) with wavenumber of 5962-5719 cm^{-1} for 80, 96.1, and 100%DD (green, purple and red, respectively).

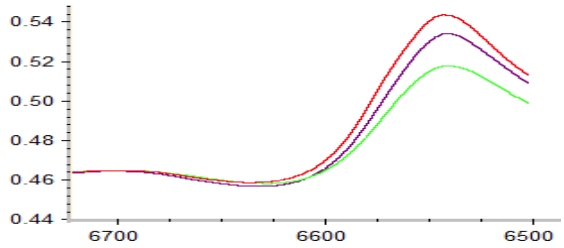

Figure 3-5: N-H (1st overtone) with wavenumber of 6841-6605 cm-1 for 80, 96.1, and 100% DD (green, purple, and red, respectively).

A comparison of actual and predicted values and residual error (Figure 6) indicated an excellent prediction of DD of powdered samples using the integrated sphere module, with a standard deviation of 0.192 %DD and a 95% confidence interval of ±0.055% DD. Since the DD was determined by a number of different traditional methods, it is worthwhile comparing the NIR method to the traditional methods (acid-base and potentiometric titration, UV/Vis). Typical error associated with traditional methods of determining the DD range from ±0.7 for acid-base titration to ±0.4 for Potentiometric titration, to ±0.3 for UV/Vis (Yuan et al, 2011). For the four samples tested in this work the average standard deviation was 0.190.

In order to test the result, Heterogeneous samples (Table 3-2) were applied, and the standard deviation of the measurements obtained was 0.877.

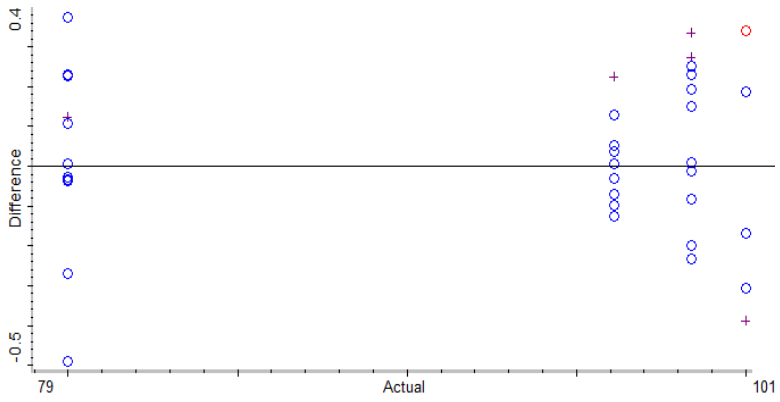

Figure 3-6: Residual for chitosan.

Table 3-2: Calculated and predicted DD of heterogeneous samples.

	Content	Calculated DD	Predicted DD
Sample A	(0.0548 gm of 80%) & (0.1441 gm of 98.4%).	91.41	91.7
Sample B	(0.0843 gm of 80%) & (0.1755 gm of 96.1).	88.37	89.7
Sample C	(0.1505gm of 96.1) & (0.3388 gm of 98.4%).	97.378	96.7
Sample D	Mixture of C (0.1092 gm) & B (0.0587 gm).	94.106	94.2
Sample E	Mixture of C (0.2934 gm) & A (0.2661 gm).	94.12	95.1

However, assuming that our samples are heterogeneous powder perfectly mixed the actual error associated with the measurements is ±0.25. Figure 3-7 shows a liner correlation between heterogeneous and homogeneous samples. Where in Figure 3-8 illustrates direct comparison of NIR with another recently reported spectroscopy method. Zajac et al (2014) recently carried out a similar study on six dried samples of known DD (70, 75, 80, 85, 90, 95%) using IR measurements at multiple wavelengths (similar to this study). The observed margin error of IR method was typically greater than 1% DD, suggesting that NIR offers some advantage over IR techniques when determining DD.

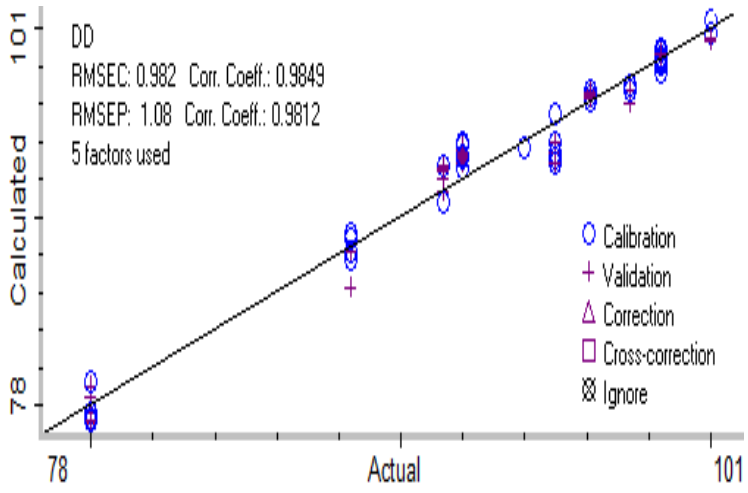

Figure 3-7: Correlation between heterogeneous and homogeneous samples.

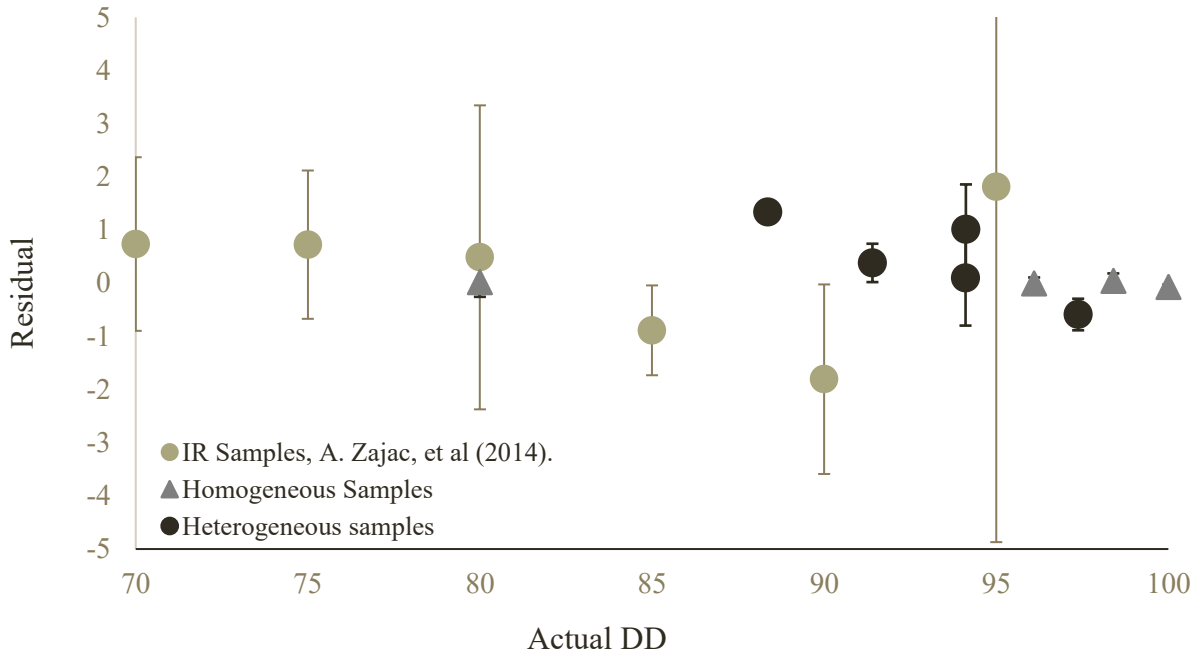

Figure 3-8: Comparison plot among IR samples, homogeneous and heterogeneous samples.

3.3 Conclusion

In this study, the DD was successfully determined by NIR spectroscopy of Chitosan in powder form. The residual error in this calibration was ±0.4% DD. These analyses were performed in seconds where no need for prior preparation for the samples, and appeared tolerant of variability in sample preparation and placement. This study is an improvement relative to traditional methods of analysis. Moreover, the samples are analyzed non-destructively; thus, any items that have been analyzed can be reused.

4 Summary & Conclusion

The aim of this thesis was to review NIR publications in a variety of research areas to assess the minimum concentrations that NIR spectroscopy has successfully detected as a precise analytical tool. As part of this objective, NIR spectroscopy was used to characterize the degree of deaetylation of chitosan powder to confirm practical accuracy in the lab and better understand the analytical method.

An extensive review of NIR applications published in food industry, agriculture, beverage analysis, and other research fields was conducted. The result reveals that FT-NIR can accurately measure moisture, sugar, protein, and other compounds provided anharmonic bonds are present or undergoes a detectable change as part of the application being monitored. Of the key application areas reviewed, NIR could be used to determine concentrations accurately at both low (10 to 100 ppm) and for the bulk phase (>50 wt%). The typical accuracy ranged from errors of 10's of ppm for select applications to more commonly SEC's of 0.1 to 1%. There was limited literature which would suggest accuracy in the sub-ppm concentration region.

The third chapter specifically focuses on evaluating the accuracy of NIR spectroscopy by conducting an experiment to characterize the degree of deacetylation (DD) of chitosan samples with different DD. The calibration and the residual plots demonstrates an excellent correlation, with standard error's consistent with the ranges observed in Chapter 2. The developed method was capable of determining average DD's for heterogeneous samples prepared from powder standards, demonstrating the advantage of NIR's increased measurement depth for bulk composition analysis of powders. When compared to other spectroscopic methods reported in literature, the standard error of the developed method appeared to represent an improvement and will be employed in future work requiring base-line measurement of DD in chitosan applications.

References

Application Bulletin 409. (2013). Analysis of chemicals using near-infrared spectroscopy. *Metrohim NIRSystem.*

Baer, I. Gurny, R., & Margot, P. (2007). NIR analysis of cellulose and lactose—Application to ecstasy tablet analysis. *Forensic Science International,* 167(2), 234-241.

Bázár, G. Romvári, R. Szabó, A. Somogyi, T. Éles, V. Tsenkova, R. (2015). NIR detection of honey adulteration reveals differences in water spectral Pattern. *Food Chemistry,* 194, 873–880.

Biniaś, W. Biniaś, D. (2014). Application of FTNIR Spectroscopy for Evaluation of the Degree of Deacetylation of Chitosan Fibres. FIBRES & TEXTILES in Eastern Europe, 23, 2(110).

Burns, D. & Ciurczak , E. (2008). HandBook of Near-Infrared Analysis 3d ed. *Scitech Book News, 32*(1).

Burke, J. (1997). IR spectroscopy or "Hooke's law at the molecular level. American Chemical Society, 74(10).

Budinova, G. Dominak, L. Strother, T., & Madison. (2008). FT-NIR Analysis of Czech Republic Beer: A Qualitative and Quantitative Approach. *Thermo Fisher scientific*.

Büning-Pfaue, H. (2003). Analysis of water in food by near infrared spectroscopy. *Food Chemistry*, 82(1), 107–115.

Cai, J. Chen, Q. Wan, X. & Zhao,J. (2011). Determination of total volatile basic nitrogen (TVB-N) content and Warner–Bratzler shear force (WBSF) in pork using Fourier transform near infrared (FT-NIR) spectroscopy. *Food Chemistry, 126*(3), 1354-1360.

Collell, C. Gou, P. Picouet, P. Arnau, J., & Comaposada, J. (2010). Feasibility of near-infrared spectroscopy to predict a w and moisture and NaCl contents of fermented pork sausages. *Meat Science, 85*(2), 325-330.

Cai, R. Wang, S. Meng, Y. Meng Q., & Zhao, W. (2012). Rapid quantification of flavonoids in propolis and previous study for classification of propolis from different origins by using near infrared spectroscopy. *Analytical Methods,4*(8), 2388-2395.

Cantor, S., Hoag, L., Ellison, S., Khan, W., & Lyon, C. (2011). NIR Spectroscopy Applications in the Development of a Compacted Multiparticulate System for Modified Release. *AAPS PharmSciTech, 12*(1), 262-278.

Clancy, Ph. (2010). Technical Note 13: Calibration of NIR Instruments. NIR Technology system.

Chauchard, Cogdill, Roussel, Roger, & Bellon-Maurel. (2004). Application of LS-SVM to non-linear phenomena in NIR spectroscopy: Development of a robust and portable sensor for acidity prediction in grapes. *Chemometrics and Intelligent Laboratory Systems, 71*(2), 141-150.

Chen, S. Danao, M. Singh, V., & Brown, P. (2014). Determining sucrose and glucose levels in dual-purpose sorghum stalks by Fourier transform near infrared (FT-NIR) spectroscopy. *Journal of the Science of Food and Agriculture, 94*(12), 2569-2576.

Costa, N., Amaral, S., Alvim, R., Nogueira, M., Schwanninger, M., & Rodrigues, J. (2013). Assessment of resin formulations and determination of the formaldehyde to urea molar ratio by near- and mid-infrared spectroscopy and multivariate data analysis. *Journal of Applied Polymer Science, 128*(1), 498-508.

Coates, J. (1998). Vibrational Spectroscopy: Instrumentation for Infrared and Raman Spectroscopy. *Applied Spectroscopy Reviews*, 33(4), 267-425.

Delwiche, S., Graybosch, R., St Amand, P., & Bai, G. (2011). Starch waxiness in hexaploid wheat (Triticum aestivum L.) by NIR reflectance spectroscopy. *Journal of Agricultural and Food Chemistry, 59*(8), 4002-8.

Enjalbert, N. Tams, C. (2009). The Use of UV/Vis/NIR Spectroscopy in the Development of Photovoltaic Cells, UV/Vis/NIR Spectroscopy. *PerkinElmer for the better.*

Frensh, R. (2010). The History of Infrared Spectroscopy. *Swinburne Astronomy Online*.

Joel, B. Warren, H. Betsy, C., & Youling Y. (2011). Deacetylation of Chitosan: Material Characterization and in vitro Evaluation via Albumin Adsorption and Pre-Osteoblastic Cell Cultures. *Materials, 4*(8), 1399-1416.

Hirsch, J. Tenkl, L., & Martin. (2013). FT-NIR Analysis of Wine. Thermo Fisher scientific.

Ingle, P., Christian, R., Purohit, P., Zarraga, V., Handley, E., Freel, K., & Abdo, S. (2016). Determination of Protein Content by NIR Spectroscopy in Protein Powder Mix Products. *Journal of AOAC International, 99*(2), 360-3.

Kumirska, J. Weinhold, M. Thöming, J. & Stepnowski, P. (2011). Biomedical Activity of Chitin/Chitosan Based Materials—Influence of Physicochemical Properties Apart from Molecular Weight and Degree of N-Acetylation. *Polymers,* 3, 1875-1901.

Magwaza, L., Opara, S., Nieuwoudt, U., Cronje, L., Saeys, H., & Nicolaï, P. (2012). NIR Spectroscopy Applications for Internal and External Quality Analysis of Citrus Fruit—A Review. *Food and Bioprocess Technology, 5*(2), 425-444.

Martin, R. (2008). Near Infrared Transmission Spectroscopy in the Food Industry.

Mehrotra, R. Gupta, A., & Nagarajan, R. (2005). NIR Spectroscopy and Fiber Optic Probe for Determination of Alcohol, Sugar and Tartaric Acid in Acoholic Beverages. *Journal of Scientific & Industrial Research*, 64,134-137.

McGoverin, C., & Manley, M. (2012). Classification of maize kernel hardness using near infrared hyperspectral imaging, *J. Near Infrared Spectrosc*. 20, 529–535.

Miller, C. (2011). Chemical Principles of Near-infrared Technology. *DuPont Engineering Technology*.

Momin, N. (2008). Chitosan and Improved Pigment Ink Jet Printing on Textiles.

Owen, T. (2000). Fundamentals of Modern UV-visible Spectroscopy. *Agilent Technologies*, P (22-23).

Nørgaard, L. et al. (2012). Principal Component Analysis and Near Infrared Spectroscopy. *Foss*, P 2-3.

Pasquini, C. (2003). Near Infrared Spectroscopy: Fundamentals, practical aspects and analytical applications. *Journal of the Brazilian Chemical Society, 14*(2), 198-219.

Páscoa, Magalhães, & Lopes. (2013). FT-NIR spectroscopy as a tool for valorization of spent coffee grounds: Application to assessment of antioxidant properties. *Food Research International, 51*(2), 579-586.

Paz, J., Visconti, M., Chiaravalle, F., & Quiñones, M. (2016). Determination of persimmon leaf chloride contents using near-infrared spectroscopy (NIRS). *Analytical and Bioanalytical Chemistry, 408*(13), 3537-3545.

Peter, L. (2011). Introduction: Infrared and Raman Spectroscopy: Principle and spectral interpretation. *26*(5). ISBN: 9780123869845.

Phan-Thien, K., Golic, M., Wright, G., & Lee, C. (2011). Feasibility of estimating peanut essential minerals by near infrared reflectance spectroscopy. *Sensing and Instrumentation for Food Quality and Safety, 5*(1), 43-49.

Purnomoadi, A. K. Batajoo, K. Ueda, K., & Terada, F. (1999 Influence of feed source on determination of fat and protein in milk by near-infrared spectroscopy. *International Dairy Journal, 9*(7), 447-452.

Rinnan, R., & Rinnan, A. (2007). Application of near infrared reflectance (NIR) and fluorescence spectroscopy to analysis of microbiological and chemical properties of arctic soil. *Soil Biology &amp, 39*, 1664-1673.

Rodriguez-Saona, L. Fry, F. McLaughlin, M., & Calvey, E. (2001). Rapid analysis of sugars in fruit juices by FT-NIR spectroscopy. *Carbohydrate Research, 336*(1), 63-74.

Roggo, Y. Chalus P. Maurer, L. Lema-Martinez, C. Edmond, A. & Jent, N. (2007). A review of near infrared spectroscopy and chemometrics in pharmaceutical technologies. *Journal of Pharmaceutical and Biomedical Analysis*, 44 (3) 683–700.

Sakudo, A. (2016). Near-infrared spectroscopy for medical applications: Current status and future perspectives. *Clinica Chimica Acta, 455*, 181-188.

Salguero-Chaparro, L. Baeten, V. Fernández-Pierna, Peña-Rodríguez, F. (2013). Near infrared Spectroscopy (NIRS) for On-line Determination of Quality Parameters in Intact Olives. *Food Chemistry*,139 (1-4), 1121–1126.

Standard, J. (2015). Introduction to Molecular Vibrations and Infrared Spectroscopy.

Stuart, B. (2004). Infrared Spectroscopy: Fundamentals and Applications. Analytical Techniques in The Sciences. *Wiley*. ISBN: 978-0-470-85428-0.

Tewari, J. Dixit, V. Cho, B., & Malikc, K. (2008). Determination of origin and sugars of citrus fruits using genetic algorithm, correspondence analysis and partial least square combined with fiber optic NIR spectroscopy. *Spectrochimica Acta Part A: Molecular and Biomolecular Spectroscopy, 71*(3), 1119-1127.

Thermo Fisher scientific. (2013). Acid and Alcohol NIR Analysis as Examples of Food Process Control. Retrieved on 03-10-2013 from https://www.thermofisher.com/ca/en/home/industrial/spectroscopy-elemental-isotope-analysis/spectroscopy-elemental-isotope-analysis-learning-center/molecular-spectroscopy-information/nir-technology/nir-food-beverage-applications.html.

Watanabe, K. D. Mansfield, S., & Avramidis, S. (2011). Application of Near-infrared Spectroscopy for Moisture-based Sorting of Green Hem-fir timber. *The Japan Wood Research Society,* 57(4), 288–294.

Xiaoying, N. Zhilei, Z. Kejun, J. Xiaoting, L. (2012). A feasibility study on quantitative analysis of glucose and fructose in lotus root powder by FT-NIR spectroscopy and chemo metrics. *Food Chemistry*, 133, 592–597.

Yang, H. & Hon, M. (2010). The Effect of the Degree of Deacetylation of Chitosan Nanoparticles and its Characterization and Encapsulation Efficiency on Drug Delivery. *Polymer-Plastics Technology and Engineering*, 49(12), 1292-1296.